Vietnam Journal of Science and Technology ***58*** *(3) (2020) 379-389*
doi:10.15625/2525-2518/58/3/14500

FREE VIBRATION ANALYSIS OF POROUS NANOPLATES USING NURBS FORMULATIONS

Phung Van Phuc[1, *], Chau Nguyen Khanh[2], Chau Nguyen Khai[2], Nguyen Xuan Hung[2]

[1]*Faculty of Civil Engineering, Ho Chi Minh City University of Technology (HUTECH), 475A Dien Bien Phu, Ho Chi Minh City, Viet Nam*

[2]*CIRTECH Institute, Ho Chi Minh City University of Technology (HUTECH), 475A Dien Bien Phu, Ho Chi Minh City, Viet Nam*

[*]Email: *pv.phuc86@hutech.edu.vn*

Received: 15 October 2019; Accepted for publication: 5 February 2020

Abstract. This paper presents free vibration analysis of functionally graded (FG) porous nanoplates based on isogeometric approach. Based on a modified power-law function, material properties are given. The nonlocal elasticity is used to capture size effects. According to a combination of the Hamilton's principle and the higher order shear deformation theory, the governing equations of the porous nanoplates are derived. Effects of nonlocal parameter, porosity volume fraction, volume fraction exponent and porosity distributions on free vibration analysis of the porous nanoplates are performed and discussed.

Keywords: porosities; nonlocal theory; nanostructures; isogeometric analysis (IGA); free vibration analysis.

Classification numbers: 2.9.2, 2.9.4, 5.4.5.

1. INTRODUCTION

New materials in Industry 4.0 play an important role and a lot of scientists have paid attention to invention. Metal foams with porosities are one of the important categories of lightweight materials. The porous volume fraction usually causes a smooth change in mechanical properties. This material plays an important role in biomedical applications. Almost researchers consider functionally graded materials (FGM) without pores, but in real structures there are several pores or voids. To make a general view in materials science, the authors try to fill this gap by studying porous FGMs.

With a high demand in engineering, especially in biomechanical applications, study on the

porous functionally graded material (PFGM) structures has attracted researchers. Based on classical plate theory (CPT), free vibration analysis of FG nanoplate using finite element method was reported in Ref. [1]. Natural frequencies of FG nanobeams [2] was also investigated. Free and forced vibrations of shear deformable functionally graded porous beams were performed by Chen *et al*. [3]. Using an analytical approach, natural frequencies of functionally graded plates with porosities via a simple four variable plate theory [4] were introduced. Buckling analysis of FG nanobeams [5] was conducted. Barati *et al*. [6] used a refined four-variable plate to study thermal buckling analysis of FG nanoplates. Besides, vibration and buckling analyses of FGM nanoplates using a new quasi 3D nonlocal theory was examined in Ref. [7]. Exact solutions of free vibration and buckling behaviors of the FG nanoplate [8] were studied. Static, buckling and free vibration analyses of nanobeam [9] were reported. Post-buckling analysis of nanoplates with porosities using analytical solutions [10] was introduced. Recently, Phung-Van [11 - 13] investigated size-dependent analysis of FG CNTRC nanoplates [11, 13] and functionally graded nanoplates [12]. Vibration analysis of FG porous nanoplates with attached mass using analytical methods [14] was performed.

As we see, a few papers related to porous nanoplates were published, and almost previous studies on porous nanoplates only used analytical solutions. Therefore, this paper aims to fill in this gap by analyzing FG porous nanoplate using non-uniform rational B-spline (NURBS) formulations. Based on the nonlocal theory of Eringen, free vibration size-dependency analysis of the porous nanoplate are investigated. Effects of nonlocal parameter, porosity volume fraction and porosity distributions on free vibration analysis of the porous nanoplates are studied and discussed in detail.

2. MATHEMATICAL FORMULATION

2.1. Nonlocal continuum theory

Based on the Eringen nonlocal theory [15], the stress can be given as:

$$\left(1-\mu\nabla^2\right)t_{ij} = \sigma_{ij} \tag{1}$$

where μ is a nonlocal parameter,

$$\nabla^2 = \partial^2/\partial x^2 + \partial^2/\partial y^2$$

is the Laplace operator; t_{ij} is the stress tensor; σ_{ij} is the local stress tensor.

A weak form for non-local elastic can be expressed as:

$$\int_V \sigma_{ij}\delta\varepsilon_{ij}\mathrm{d}V + \int_V \left(1-\mu\nabla^2\right)\rho\ddot{u}_i\delta u_i\mathrm{d}V = \int_V f_i\left(\delta u_i - \mu\nabla^2\delta u_i\right)\mathrm{d}V + \int_\Gamma \sigma_{ij}n_i\delta u_i\mathrm{d}\Gamma \tag{2}$$

2.2. Porous FG materials

A nanoplate with length a, width b and thickness h, as shown in Figure 1, is considered. Two porosity distributions including even porosities (PFGM-I) and uneven porosities (PFGM-II) are studied. Porosities in PFGM-I are randomly distributed through the thickness. While for PFGM-II, porosities are distributed around middle zone.

Based on the modified rule of mixture, the material properties, $P(z)$, in z-direction of PFGM are defined as:

$$P(z) = P_c\left(V_c - \frac{\xi}{2}\right) + P_m\left(V_m - \frac{\xi}{2}\right) \tag{3}$$

where ξ is porosity volume fraction; V_c and V_m are volume fractions of ceramic and metal defined as:

$$V_m + V_c = 1 \quad , \quad V_c = \left(\frac{1}{2} + \frac{z}{h}\right)^n \tag{4}$$

in which n represents volume fraction exponent; c and m are ceramic and metal, respectively.

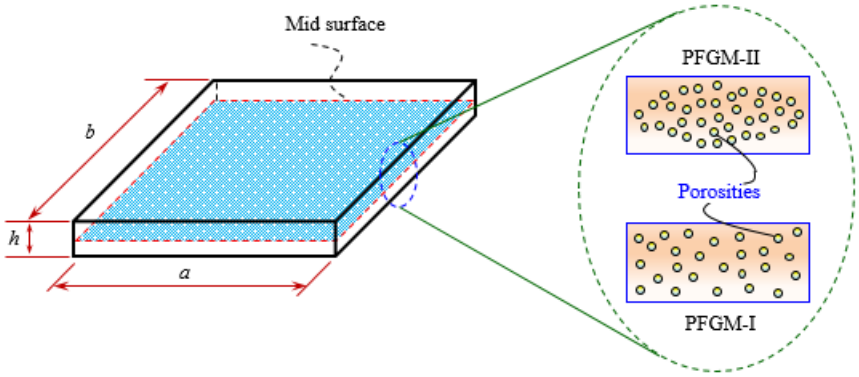

Figure 1. Two porosity distributions.

Material properties of PFGM are expressed [6, 7]:

$$\begin{aligned} P(z) &= (P_c - P_m)V_c + P_m - (P_c + P_m)\frac{\xi}{2} \quad \text{for PFGM-I} \\ P(z) &= (P_c - P_m)V_c + P_m - (P_c + P_m)\frac{\xi}{2}\left(1 - \frac{2|z|}{h}\right) \quad \text{for PFGM-II} \end{aligned} \tag{1}$$

The expressions of Young's modulus, density, Poisson's ratio can be given as

$$\text{for PFGM-I} \begin{cases} E(z) = (E_c - E_m)V_c + E_m - (E_c + E_m)\dfrac{\xi}{2} \\ \nu(z) = (\nu_c - \nu_m)V_c + \nu_m - (\nu_c + \nu_m)\dfrac{\xi}{2} \\ \rho(z) = (\rho_c - \rho_m)V_c + \rho_m - (\rho_c + \rho_m)\dfrac{\xi}{2} \end{cases}$$

$$\text{for PFGM-II} \begin{cases} E(z) = (E_c - E_m)V_c + E_m - (E_c + E_m)\dfrac{\xi}{2}\left(1 - \dfrac{2|z|}{h}\right) \\ \nu(z) = (\nu_c - \nu_m)V_c + \nu_m - (\nu_c + \nu_m)\dfrac{\xi}{2}\left(1 - \dfrac{2|z|}{h}\right) \\ \rho(z) = (\rho_c - \rho_m)V_c + \rho_m - (\rho_c + \rho_m)\dfrac{\xi}{2}\left(1 - \dfrac{2|z|}{h}\right) \end{cases} \quad (2)$$

Young's modulus distributions of porous nanoplate made of Al/ZrO2-1 are plotted in Figure 2. Effect of porosities on Young's modulus is also shown in Figure 2b and Figure 2c. Forms of curves of Young's modulus of PFGM-I are the same as those of FGM with a decrease in Young's modulus amplitude. Besides, it is observed that Young's modulus of PFGM-II is maximum at the top and the bottom and decreases towards middle zone direction, as indicated in Figure 2d.

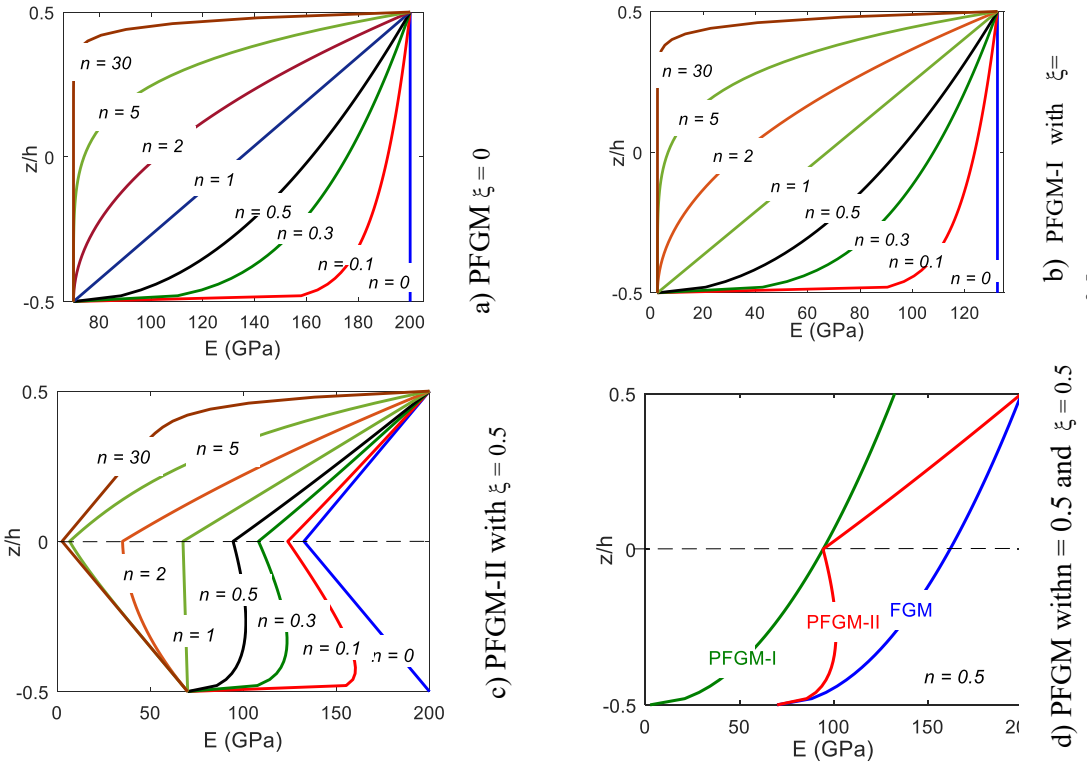

Figure 2. Young's modulus of porous Al/ZrO2-1: (a) PFGM $\xi = 0$, (b) PFGM-I with $\xi = 0.5$, (c) PFGM-II with $\xi = 0.5$, (d) PFGM-II with $\xi = 0.5$.

2.3. Higher order shear deformation theory

The displacement field of the porous nanoplate can be defined:

$$\begin{aligned} u(x,y,z) &= u_0(x,y) - z\frac{\partial w}{\partial x} + f(z)\beta_x(x,y) \\ v(x,y,z) &= v_0(x,y) - z\frac{\partial w}{\partial y} + f(z)\beta_y(x,y) \\ w(x,y,z) &= w_0(x,y) \end{aligned} \tag{3}$$

where u_0, v_0 and w_0 are the displacements in plane and deflection; β_x and β_y are rotations;

$$f(z) = z - \tfrac{4}{3h^2}z^3.$$

The strains of the nanoplate can be formulated:

$$\boldsymbol{\varepsilon} = \begin{bmatrix} \varepsilon_{xx} \\ \varepsilon_{yy} \\ \varepsilon_{xy} \end{bmatrix} = \begin{bmatrix} \dfrac{\partial u}{\partial x} \\ \dfrac{\partial v}{\partial y} \\ \dfrac{\partial u}{\partial y} + \dfrac{\partial v}{\partial x} \end{bmatrix} = \begin{bmatrix} \dfrac{\partial u_0}{\partial x} \\ \dfrac{\partial v_0}{\partial x} \\ \dfrac{\partial u_0}{\partial y} + \dfrac{\partial v_0}{\partial x} \end{bmatrix} + z\begin{bmatrix} -\dfrac{\partial^2 w}{\partial x^2} \\ -\dfrac{\partial^2 w}{\partial y^2} \\ -2\dfrac{\partial^2 w}{\partial x \partial y} \end{bmatrix} + f(z)\begin{bmatrix} \dfrac{\partial \beta_x}{\partial x} \\ \dfrac{\partial \beta_y}{\partial y} \\ \dfrac{\partial \beta_x}{\partial y} + \dfrac{\partial \beta_y}{\partial x} \end{bmatrix} \tag{4}$$

$$\boldsymbol{\gamma} = \begin{bmatrix} \gamma_{xz} \\ \gamma_{yz} \end{bmatrix} = \begin{bmatrix} \dfrac{\partial u}{\partial z} + \dfrac{\partial w}{\partial x} \\ \dfrac{\partial v}{\partial z} + \dfrac{\partial w}{\partial y} \end{bmatrix} = f'(z)\begin{bmatrix} \beta_x \\ \beta_y \end{bmatrix} \tag{5}$$

Equation (4) can be rewritten in a shorter form:

$$\boldsymbol{\varepsilon} = \boldsymbol{\varepsilon}_m + z\boldsymbol{\kappa}_1 + f(z)\boldsymbol{\kappa}_2 \;\; ; \;\; \boldsymbol{\gamma} = f'(z)\boldsymbol{\varepsilon}_s \tag{6}$$

where

$$\boldsymbol{\varepsilon}_m = \begin{bmatrix} u_{0,x} \\ v_{0,y} \\ u_{0,y} + v_{0,x} \end{bmatrix} ; \; \boldsymbol{\kappa}_1 = \begin{bmatrix} -w_{0,xx} \\ -w_{0,yy} \\ -2w_{0,xy} \end{bmatrix} ; \; \boldsymbol{\kappa}_2 = \begin{bmatrix} \beta_{x,x} \\ \beta_{y,y} \\ \beta_{x,y} + \beta_{y,x} \end{bmatrix} ; \; \boldsymbol{\varepsilon}_s = \begin{bmatrix} \beta_x \\ \beta_y \end{bmatrix} \tag{7}$$

The stresses based on Hooke's law can be defined:

$$\begin{aligned} \boldsymbol{\sigma} &= \begin{pmatrix} \sigma_{xx} & \sigma_{yy} & \sigma_{xy} \end{pmatrix}^T = \mathbf{C}_b\boldsymbol{\varepsilon} = \mathbf{C}_b\left(\boldsymbol{\varepsilon}_m + z\boldsymbol{\kappa}_1 + f(z)\boldsymbol{\kappa}_2\right) \\ \boldsymbol{\tau} &= \begin{pmatrix} \tau_{xz} & \tau_{yz} \end{pmatrix}^T = \mathbf{C}_s\boldsymbol{\gamma} = \mathbf{C}_s f'(z)\boldsymbol{\varepsilon}_s \end{aligned} \tag{8}$$

where

$$\mathbf{C}_b = \frac{E(z)}{1-\nu(z)^2}\begin{bmatrix} 1 & \nu(z) & 0 \\ \nu(z) & 1 & 0 \\ 0 & 0 & \frac{1-\nu(z)}{2} \end{bmatrix} \;\; ; \;\; \mathbf{C}_s = \frac{E(z)}{2(1+\nu(z))}\begin{bmatrix} 1 & 0 \\ 0 & 1 \end{bmatrix} \tag{9}$$

According to Eq. (8), the stress resultants can be expressed:

$$\left(1-\mu\nabla^2\right)\begin{Bmatrix}N_{xx}\\N_{yy}\\N_{xy}\end{Bmatrix}=\int_{-h/2}^{h/2}\begin{Bmatrix}\sigma_{xx}\\\sigma_{yy}\\\sigma_{xy}\end{Bmatrix}\mathrm{d}z\quad;\quad\left(1-\mu\nabla^2\right)\begin{Bmatrix}M_{xx}\\M_{yy}\\M_{xy}\end{Bmatrix}=\int_{-t/2}^{h/2}\begin{Bmatrix}\sigma_{xx}\\\sigma_{yy}\\\sigma_{xy}\end{Bmatrix}z\mathrm{d}z;$$
$$\left(1-\mu\nabla^2\right)\begin{Bmatrix}P_{xx}\\P_{yy}\\P_{xy}\end{Bmatrix}=\int_{-h/2}^{h/2}\begin{Bmatrix}\sigma_{xx}\\\sigma_{yy}\\\sigma_{xy}\end{Bmatrix}f(z)\mathrm{d}z\quad;\quad\left(1-\mu\nabla^2\right)\begin{Bmatrix}Q_{xz}\\Q_{yz}\end{Bmatrix}=\int_{-t/2}^{h/2}\begin{Bmatrix}\tau_{xz}\\\tau_{yz}\end{Bmatrix}f'(z)\mathrm{d}z \tag{10}$$

Substituting Eq. (8) into Eq. (10), we obtain:

$$\left(1-\mu\nabla^2\right)\begin{bmatrix}\mathbf{N}\\\mathbf{M}\\\mathbf{P}\\\mathbf{Q}\end{bmatrix}=\begin{bmatrix}\mathbf{A}&\mathbf{B}&\mathbf{E}&\mathbf{0}\\\mathbf{B}&\mathbf{D}&\mathbf{F}&\mathbf{0}\\\mathbf{E}&\mathbf{F}&\mathbf{G}&\mathbf{0}\\\mathbf{0}&\mathbf{0}&\mathbf{0}&\mathbf{A}_s\end{bmatrix}\begin{bmatrix}\boldsymbol{\varepsilon}_m\\\boldsymbol{\kappa}_1\\\boldsymbol{\kappa}_2\\\boldsymbol{\varepsilon}_s\end{bmatrix} \tag{11}$$

where

$$\left(\mathbf{A},\mathbf{B},\mathbf{D},\mathbf{E},\mathbf{F},\mathbf{G}\right)=\mathbf{C}_b\int\left(1,z,z^2,f(z),zf(z),f^2(z)\right)\mathrm{d}z\quad;\quad\mathbf{A}_s=\mathbf{C}_s\int\left[f'(z)\right]^2\mathrm{d}z \tag{12}$$

A weak form of the nanoplate can be given as:

$$\int_\Omega\left[\left(\delta\boldsymbol{\varepsilon}\right)^T\mathbf{D}_{mb}\boldsymbol{\varepsilon}+\left(\delta\boldsymbol{\gamma}\right)^T\mathbf{A}_s\boldsymbol{\gamma}\right]\mathrm{d}\Omega+\int_\Omega\delta\mathbf{u}^T\mathbf{m}\left(1-\mu\nabla^2\right)\ddot{\mathbf{u}}\mathrm{d}\Omega=\mathbf{0} \tag{13}$$

where

$$\mathbf{D}_{mb}=\begin{bmatrix}\mathbf{A}&\mathbf{B}&\mathbf{E}\\\mathbf{B}&\mathbf{D}&\mathbf{F}\\\mathbf{E}&\mathbf{F}&\mathbf{H}\end{bmatrix};\quad\mathbf{m}=\begin{bmatrix}\mathbf{I}&\mathbf{0}&\mathbf{0}\\\mathbf{0}&\mathbf{I}&\mathbf{0}\\\mathbf{0}&\mathbf{0}&\mathbf{I}\end{bmatrix};\ \mathbf{I}=\begin{bmatrix}I_1&I_2&I_4\\I_2&I_3&I_5\\I_4&I_5&I_6\end{bmatrix},$$
$$\left(I_1,I_2,I_3,I_4,I_5,I_6\right)=\int_{-h/2}^{h/2}\rho\left(1,z,z^2,f(z),zf(z),f^2(z)\right)\mathrm{d}z \tag{14}$$

and

$$\mathbf{u}=\begin{bmatrix}\mathbf{u}_1\\\mathbf{u}_2\\\mathbf{u}_3\end{bmatrix};\ \mathbf{u}_1=\begin{bmatrix}u_0\\-\dfrac{\partial w}{\partial x}\\\beta_x\end{bmatrix};\ \mathbf{u}_2=\begin{bmatrix}v_0\\-\dfrac{\partial w}{\partial y}\\\beta_y\end{bmatrix};\ \mathbf{u}_3=\begin{bmatrix}w_0\\0\\0\end{bmatrix} \tag{15}$$

3. FG POROUS NANOPLATE FORMULATION

Based on NURBS basis functions [16], the displacement field is defined as follows:

$$\mathbf{u}^h\left(\xi,\eta\right)=\sum_{I=1}^{m\times n}R_I\left(\xi,\eta\right)\mathbf{d}_I \tag{16}$$

where R_I is the NURBS basis function and $\mathbf{d}_I = \left[u_{0I}\ v_{0I}\ w_I\ \beta_{xI}\ \beta_{yI}\right]^T$ is degrees of freedom.

Substituting Eq. (16) into Eqs. (6) – (7), the strains are rewritten:

$$\boldsymbol{\varepsilon}_m = \sum_{I=1}^{m\times n} \mathbf{B}_I^m \mathbf{d}_I \ ;\ \boldsymbol{\kappa}_1 = \sum_{I=1}^{m\times n} \mathbf{B}_I^{b1} \mathbf{d}_I \ ;\ \boldsymbol{\kappa}_2 = \sum_{I=1}^{m\times n} \mathbf{B}_I^{b2} \mathbf{d}_I \ ;\ \boldsymbol{\varepsilon}_s = \sum_{I=1}^{m\times n} \mathbf{B}_I^{s} \mathbf{d}_I \tag{17}$$

where

$$\mathbf{B}_I^m = \begin{bmatrix} R_{I,x} & 0 & 000 \\ 0 & R_{I,y} & 000 \\ R_{I,y} & R_{I,x} & 000 \end{bmatrix},\ \mathbf{B}_I^{b1} = \begin{bmatrix} 00 & -R_{I,xx} & 00 \\ 00 & -R_{I,yy} & 00 \\ 00 & -2R_{I,xy} & 00 \end{bmatrix},\ \mathbf{B}_I^{b2} = \begin{bmatrix} 000 & R_{I,x} & 0 \\ 000 & 0 & R_{I,y} \\ 000 & R_{I,y} & R_{I,x} \end{bmatrix},$$
$$\mathbf{B}_I^s = \begin{bmatrix} 00\,0 & R_I & 0 \\ 00\,0 & 0 & R_I \end{bmatrix} \tag{18}$$

The governing equation for free vibration analysis is given:

$$\left(\mathbf{K} - \omega^2 \mathbf{M}\right)\mathbf{d} = \mathbf{0} \tag{19}$$

where

$$\mathbf{K} = \int_\Omega \left[\left[\mathbf{B}^m\ \mathbf{B}^{b1}\ \mathbf{B}^{b2}\right]^T \mathbf{D}_{mb} \left[\mathbf{B}^m\ \mathbf{B}^{b1}\ \mathbf{B}^{b2}\right] + \left(\mathbf{B}^s\right)^T \mathbf{A}_s \mathbf{B}^s\right] \mathrm{d}\Omega$$
$$\mathbf{M} = \int_\Omega \tilde{\mathbf{R}}^T \mathbf{m}\left(\tilde{\mathbf{R}} - \mu \nabla^2 \tilde{\mathbf{R}}\right) \mathrm{d}\Omega \tag{20}$$

with

$$\tilde{\mathbf{R}} = \begin{Bmatrix} \mathbf{R}_1 \\ \mathbf{R}_2 \\ \mathbf{R}_3 \end{Bmatrix},\ \mathbf{R}_1 = \begin{bmatrix} R_I & 0 & 0 & 0\,0 \\ 0 & 0 & -R_{I,x} & 0\,0 \\ 0 & 0 & 0 & R_I\,0 \end{bmatrix},\ \mathbf{R}_2 = \begin{bmatrix} 0 & R_I & 0 & 0\,0 \\ 0 & 0 & -R_{I,y} & 0\,0 \\ 0 & 0 & 0 & 0\,R_I \end{bmatrix},\ \mathbf{R}_3 = \begin{bmatrix} 0\,0 & R_I & 0\,0 \\ 0\,0 & 0 & 0\,0 \\ 0\,0 & 0 & 0\,0 \end{bmatrix} \tag{21}$$

From Eq. (20), the basic functions are required at least third order derivatives. So, IGA can be considered as the most suitable candidate to calculate the nanoplates with porosities.

4. NUMERICAL EXAMPLES

Some examples of porous nanoplates are performed. Table 1 lists the material properties of FGMs.

A SUS304/Si3N4 nanoplate (a = 10, a/h = 10) is studied. The frequency $\bar{\omega}$ is defined [11]:

$$\bar{\omega} = \omega h \sqrt{\frac{\rho_c}{G_c}} \ ;\ G_c = \frac{E_c}{2\left(1+\nu_c\right)} \tag{22}$$

where ω is frequency obtained by solving Eq. (19).

Table *2* shows the first two frequencies of the nanoplate without porosities. As observed that results of the proposed method match very well with reference solutions [11]. The lowest four mode shapes are shown in Figure 3.

Table 1. Material properties of FGMs.

	Al	SUS304	Al2O3	ZrO2-1	Si3N4
E	70×10^9	201.04×10^9	380×10^9	200×10^9	384.43×10^9
ν	0.3	0.3	0.3	0.3	0.3
ρ	2707	8166	3800	5700	2370

Table 2. The first two natural frequencies of a nanoplates with a = 10, a/h = 10 and $\xi = 0$.

n	Model	Mode 1				Mode 2			
		μ				μ			
		0	1	2	4	0	1	2	4
2	Ref. [11]	0.0485	0.0443	0.0410	0.0362	0.1154	0.0944	0.0819	0.0669
	IGA	0.0466	0.0426	0.0395	0.0349	0.1138	0.0930	0.0806	0.0659
10	Ref. [11]	0.0416	0.0380	0.0352	0.0311	0.0990	0.0810	0.0702	0.0574
	IGA	0.0400	0.0365	0.0338	0.0299	0.0975	0.0797	0.0691	0.0564

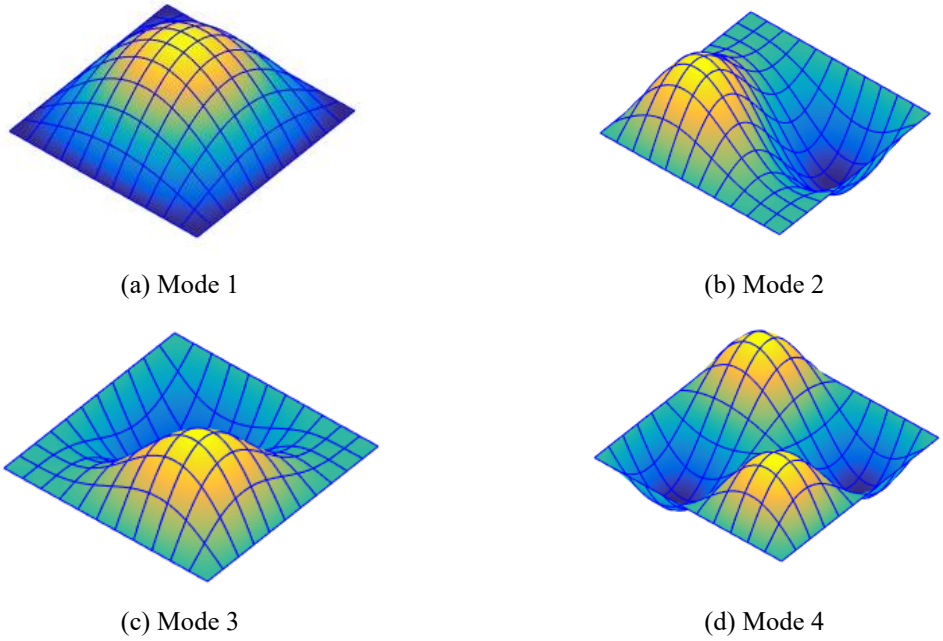

(a) Mode 1 (b) Mode 2

(c) Mode 3 (d) Mode 4

Figure 3. The lowest four mode shapes of a porous nanoplate.

Next, the first six frequencies of the nanoplate made of Al/Al2O3 with simply supported (SSSS) and clamped (CCCC) boundary conditions are listed in Table 3 and Table 4, respectively. We see that when porous parameter increases, the frequencies increase. This is because when the nonlocal parameter increases, the stiffness of the plate increases as well.

Table 3. The six lowest frequencies of the SSSS Al/Al2O3 with n = 3.

μ	ξ	Type	Mode					
			1	2	3	4	5	6
0	0.0	FGM	0.0599	0.1456	0.1456	0.2127	0.2128	0.2234
	0.1	PFGM-I	0.0554	0.1350	0.1350	0.2060	0.2061	0.2075
		PFGM-II	0.0592	0.1437	0.1438	0.2099	0.2099	0.2205
	0.2	PFGM-I	0.0485	0.1183	0.1183	0.1823	0.1939	0.1939
		PFGM-II	0.0584	0.1414	0.1414	0.2062	0.2062	0.2168
	0.3	PFGM-I	0.0346	0.0845	0.0845	0.1311	0.1619	0.1628
		PFGM-II	0.0572	0.1382	0.1382	0.2013	0.2013	0.2118
1	0.0	FGM	0.0547	0.1191	0.1191	0.1668	0.1944	0.1955
	0.1	PFGM-I	0.0506	0.1104	0.1104	0.1548	0.1809	0.1820
		PFGM-II	0.0541	0.1176	0.1176	0.1646	0.1916	0.1928
	0.2	PFGM-I	0.0443	0.0968	0.0968	0.1361	0.1594	0.1604
		PFGM-II	0.0533	0.1156	0.1157	0.1618	0.1879	0.1892
	0.3	PFGM-I	0.0316	0.0691	0.0691	0.098	0.1148	0.1155
		PFGM-II	0.0523	0.1130	0.1130	0.1581	0.1831	0.1844
2	0.0	FGM	0.0507	0.1032	0.1032	0.1388	0.1589	0.1598
	0.1	PFGM-I	0.0469	0.0957	0.0957	0.1289	0.1478	0.1487
		PFGM-II	0.0501	0.1019	0.1019	0.1370	0.1566	0.1575
	0.2	PFGM-I	0.0411	0.0839	0.0839	0.1134	0.1302	0.1310
		PFGM-II	0.0494	0.1002	0.1002	0.1347	0.1536	0.1546
	0.3	PFGM-I	0.0293	0.0599	0.0599	0.0816	0.0939	0.0944
		PFGM-II	0.0484	0.0980	0.0980	0.1316	0.1496	0.1507

Table 4. The first six frequencies of the CCCC Al/Al2O3 nanoplates with n = 3.

μ	ξ	Type	Mode					
			1	2	3	4	5	6
0	0.0	FGM	0.1091	0.2091	0.2092	0.3013	0.3446	0.3479
	0.1	PFGM-I	0.1014	0.1950	0.1951	0.2811	0.3227	0.3256
		PFGM-II	0.1078	0.2062	0.2064	0.2971	0.3393	0.3426
	0.2	PFGM-I	0.0891	0.1722	0.1723	0.2482	0.2870	0.2895
		PFGM-II	0.1061	0.2025	0.2026	0.2916	0.3324	0.3357
	0.3	PFGM-I	0.0635	0.1243	0.1244	0.1791	0.2108	0.2123
		PFGM-II	0.1037	0.1974	0.1976	0.2842	0.3232	0.3265
1	0.0	FGM	0.0981	0.1671	0.1672	0.2194	0.2380	0.2412
	0.1	PFGM-I	0.0911	0.1556	0.1557	0.2043	0.2226	0.2254
		PFGM-II	0.0969	0.1648	0.1649	0.2163	0.2343	0.2374

	0.2	PFGM-I	0.0799	0.1372	0.1373	0.1800	0.1975	0.1999
		PFGM-II	0.0953	0.1617	0.1619	0.2122	0.2295	0.2326
	0.3	PFGM-I	0.0569	0.0986	0.0986	0.1290	0.1440	0.1456
		PFGM-II	0.0932	0.1577	0.1579	0.2068	0.2232	0.2262
2	0	FGM	0.0898	0.1430	0.1431	0.1808	0.1927	0.1958
	0.1	PFGM-I	0.0833	0.1332	0.1333	0.1683	0.1801	0.1830
		PFGM-II	0.0887	0.1410	0.1412	0.1782	0.1897	0.1928
	0.2	PFGM-I	0.0731	0.1173	0.1173	0.1481	0.1597	0.1621
		PFGM-II	0.0872	0.1385	0.1386	0.1749	0.1858	0.1889
	0.3	PFGM-I	0.0519	0.0841	0.0841	0.1059	0.1162	0.1179
		PFGM-II	0.0853	0.1350	0.1351	0.1704	0.1807	0.1837

4. CONCLUSIONS

Free vibration analysis of the nanoplates with porosities using IGA was introduced. The nonlocal theory was used to examine size effects. Based on the present formulations numerical results, it can be withdrawn some points:

IGA is a suitable candidate to analyze the porous nanoplates.

Free frequency of PFGM-II is larger than that of PFGM-I.

When porous parameter rises, frequencies increases.

Acknowledgements. This research is funded by Vietnam National Foundation for Science and Technology Development (NAFOSTED) under grant number 107.02-2019.09.

REFERENCES

1. Natarajan S., Chakraborty S., Thangavel M., Bordas S., Rabczuk T. - Size-dependent free flexural vibration behavior of functionally graded nanoplates, Comp. Mater. Sci. **65** (2012) 74-80.
2. Alshorbagy A. E., Eltaher M. A., Mahmoud F. F. - Free vibration characteristics of a functionally graded beam by finite element method, Appl. Math. Model **35** (1) (2011) 412-25.
3. Chen D., Yang J., Kitipornchai S. - Free and forced vibrations of shear deformable functionally graded porous beams, International Journal of Mechanical Sciences **108** (2016) 14-22.
4. Rezaei A., Saidi A., Abrishamdari M., Mohammadi M. P. - Natural frequencies of functionally graded plates with porosities via a simple four variable plate theory: an analytical approach, Thin-Walled Structures **120** (2017) 366-77.
5. Eltaher M. A., Emam S. A., Mahmoud F. F. - Static and stability analysis of nonlocal functionally graded nanobeams, Compos Struct. **96** (2013) 82-8.
6. Barati M. R., Shahverdi H. - A four-variable plate theory for thermal vibration of embedded FG nanoplates under non-uniform temperature distributions with different boundary

conditions, Struct. Eng. Mech. **60** (4) (2016) 707-27.

7. Sobhy M., Radwan A. F. - A New Quasi 3D Nonlocal Plate Theory for Vibration and Buckling of FGM Nanoplates, Int. J. Appl. Mech. **9** (1) (2017) 1750008.
8. Ansari R., Ashrafi M., Pourashraf T., Sahmani S. - Vibration and buckling characteristics of functionally graded nanoplates subjected to thermal loading based on surface elasticity theory, Acta Astronaut. **109** (2015) 42-51.
9. Thai H. T. - A nonlocal beam theory for bending, buckling, and vibration of nanobeams, Int J Eng Sci. **52** (2012) 56-64.
10. Barati M. R., Zenkour A. M. - Analysis of postbuckling behavior of general higher-order functionally graded nanoplates with geometrical imperfection considering porosity distributions, Mechanics of Advanced Materials and Structures **26** (2019) 1081-1088.
11. Phung-Van P., Lieu Q. X., Nguyen-Xuan H., Wahab M. A. - Size-dependent isogeometric analysis of functionally graded carbon nanotube-reinforced composite nanoplates, Compos Struct. **166** (2017) 120-35.
12. Phung-Van P., Ferreira A. J. M., Nguyen-Xuan H., Abdel-Wahab M. - An isogeometric approach for size-dependent geometrically nonlinear transient analysis of functionally graded nanoplates, Composites Part B Engineering **118** (2017) 125-34.
13. Phung-Van P., Thanh C. L., Nguyen-Xuan H., Abdel-Wahab M. - Nonlinear transient isogeometric analysis of FG-CNTRC nanoplates in thermal environments, Composite Structures **201** (2018) 882-92.
14. Shahverdi H., Barati M. R. - Vibration analysis of porous functionally graded nanoplates. Int J Eng Sci. **120** (2017) 82-99.
15. Eringen A. C. - Nonlocal Polar Elastic Continua, Int J. Eng. Sci. **10** (1) (1972) 1-7.
16. Cottrell J. A., Hughes T. J. R., Bazilevs Y. - Isogeometric analysis, towards integration of CAD and FEA: Wiley, 2009.